Chapter 3

COORDINATE SYSTEMS AND FLUX BIAS ERROR

Xuhui Lee, John Finnigan, Kyaw Tha Paw U
xuhui.lee@yale.edu

Abstract

This Chapter examines theoretical and operational aspects of coordinate systems. A distinction is made between the vector basis, a local property of a coordinate system, and the overall coordinate frame consisting of the vector basis and coordinate lines, a global property of the flow that is determined by the flow field in three dimensions. Point measurements can only define the vector basis. Because in field campaigns many components that enter into the mass balance in complex flows are severely under-sampled, a properly chosen coordinate frame for point measurements should optimize our estimates of the surface-air exchange and should maximize information for diagnostics purposes.

The strengths and weaknesses of three operational coordinate systems for point measurements (instrument, natural wind, and planar fit) are examined in detail. Th rror in scalar fluxes due to coordinate tilt is usually small for small tilt angles does not negate the need for coordinate rotation because the tilt error can introduce a systematic bias to the time integrated flux. On the other hand, it is also important that over-rotation be avoided in post-field data analysis. Tilt errors caused by contamination from th reamwise and cross-wind fluxes should be treated differently.

Appendix B outlines a method for rotation into the planar fit coordinate. The scheme relies on the straightforward vector operation and avoids the need for rotation angles.

1 Introduction

Application of coordinate rotation is a necessary step in micrometeorological studies of surface-air exchange before the observed fluxes can be meaningfully interpreted. The most common rotation procedure

X. Lee et al. (eds.), Handbook of Micrometeorology, 33–66.

uses measured mean wind to define an orthogonal vector basis, termed natural wind system, for each observational period (e. g., 30 min) to which all fluxes are transformed. The rotation scheme is intended to level the sonic anemometer to the terrain surface. When it was first proposed by Tanner and Thurtell in 1969 [see also Kaimal and Finnigan (1994) and McMillen (1988)], the natural wind system was limited to a surface layer in which the flow is one dimensional, that is, the velocity and scalar concentration gradients exist only in the vertical and hence no horizontal scalar advection nor flow divergence, and there is no wind directional shear causing a cross-wind momentum flux. It appeared sufficient from the 1960's through the early 1990's as most field experiments then were conducted at ideal sites, over selected "golden days", and in fair weather conditions. The scope of micrometeorological research has now been extended considerably, to include non-ideal sites and year-round, continuous monitoring, and the validity of the procedure is now called into question.

More recent rotation schemes (Wilczak et al. 2001, Paw U et al. 2000, Lee 1998) attempt to overcome some of the deficiencies of the natural wind system. However, like Tanner and Thurtell (1969), they do not in fact treat coordinate systems at all but focus rather on the orientation of the vector basis, $\vec{e}_i$, in which vector and tensor quantities are to be represented. This is an important and continuing question as the circumstances of most flux sites dictate that the wind field itself must be

rient $\vec{e}_i$. The vector basis is a local property of a coordinate system but it is the global properties of the flow field that dictate the form of the mass balance equation that we employ to convert flux measurements to measures of surface exchange and so it is vital to understand the relationship between the two quantities as well as the advantages and disadvantages of different coordinate systems.

Removal of "tilt errors" or cross-contamination among components of the eddy flux vector is cited in the literature as the main reason for performing coordinate rotation. Kaimal and Haugen (1969) and others have shown that momentum flux is particularly sensitive to the tilt errors. Scalar fluxes are not as sensitive, but the errors could potentially cause a systematic bias in annually integrated eddy fluxes (Section 4). It is known that a tilt-corrected flux does not necessarily represent the true surface-air exchange because non-turbulent advective components of the surface-layer mass balance may be non-negligible even at ideal sites. A proper coordinate frame is vitally important to advance our understanding of these issues.

Strictly, to use measurements of wind speed, concentration and eddy flux to infer surface exchange of a scalar c involves the assimilation of

measurements into a description of the mass balance in a control volume V, erected over a representative patch of the surface (e. g., Figure 6.1 of Chapter 6). The mass balance of c is the sum of the fluxes of c across each face of the control volume plus the accumulation of c within the volume. If we can measure the fluxes across each aerial face as well as the rate of change of c within V, we can deduce the transfer across the surface by difference. Whatever kind of instrumentation we employ, however, we are only able to sample the aerodynamic flux and the rate of change of c at a few points in space and we are forced to either supply the missing information in other ways or develop good diagnostic tools that can aid selective use of data.

The mathematical form of the mass balance that we employ has a considerable bearing upon our ability to estimate its constituent terms from a finite number of measurements. The two main factors affecting this form are the averaging operations applied to the instantaneous variables and the coordinate system in which the mass balance is represented. The question of averaging operators and their relationship to coordinate alignment is dealt with in detail in Finnigan et al. (2003) and Sakai et al. (2001) although there, the only coordinate system considered is the familiar rectangular Cartesian frame. Here we concentrate on the choice of coordinate system and assume that an appropriate averaging operator may be applied to the measurements.

This Chapter examines theoretical and operational aspects of coordinate systems. It begins with a brief discussion of the theoretical constraints on the coordinate system. [The reader is referred to Finnigan (2004) for more details.] This is followed by a discussion on the strengths and weaknesses of three common coordinate frames for point measurements, the instrument coordinate, the natural wind system, and the planar fit coordinate (Section 3). Section 4 provides a assessment of flux bias errors due to sensor tilt in horizontally homogeneous flow. Section 5 discusses examples of coordinate tilt that are likely to occur in field observations. In Section 6, a dataset obtained over a forest in complex terrain is analyzed to examine the sensitivity of flux calculation to coordinate rotation.

2 Theory

2.1 Mass balance at a point

A coordinate frame is meaningful only if it is consistent with the frame used by equations that comprise, either explicitly or implicitly, the theory underlying the study. Kaimal and Finnigan (1994) state, "... problems occur when vector quantities like velocities or fluxes are mea-

sured in a reference framework that does not coincide with that of the equations used to analyze them". The fundamental equation for surface-air exchange studies is the mass conservation equation. Although in a strictly formal analysis, all fluxes can be expressed as 3-dimensional vectors with the gradient operator being independent of coordinate system (Massman and Lee 2002), in practice a coordinate frame is needed to estimate the surface-atmosphere exchange and the related turbulent statistics, including the net ecosystem exchange (NEE).

The statement of conservation of a scalar c at a point in an incompressible fluid is

$$\frac{\partial c}{\partial t} + \nabla.\vec{u}c = S(\vec{x})\delta(\vec{x} - \vec{x}_0) \tag{3.1}$$

where the velocity vector $\vec{u}$ has components u, v, w corresponding to position vector $\vec{x}$ with components x, y, z. The source term S is multiplied by the Dirac delta function, signifying that the source is zero except on the ground and vegetation surfaces, whose locus is $\vec{x}_0$. We have ignored molecular diffusion, which is negligible except very close to solid surfaces when its effects can be conveniently absorbed in the specification of the source strength, for example via the device of a boundary-layer resistance. The scalar c represents any absolute fluid property such as density of carbon dioxide or heat content. For alternative formulations of the mass balance see Paw U et al. (2000) and Raupach (2001).

Each term in Equation 3.1 is a scalar and so is independent of the coordinate frame. The individual components of the divergence term, however, take different forms in different coordinate systems. There are three overriding requirements guiding the choice of coordinate frame and its orientation

- We must be able to express our measurements in the chosen coordinate frame.
- Since we can rarely measure all the components of $\nabla.\vec{u}c$, we want to work in a coordinate frame that optimizes our ability to estimate $\nabla.\vec{u}c$, using the terms we can measure.
- If we want to assimilate our measurements explicitly into a mathematical model of flow and transport, we would like to be able to construct such a model in the chosen coordinates.

In this Chapter we consider only the first two of these requirements.

We can illustrate the dependence of the form of the flux divergence upon coordinate frame and orientation most simply through the example of one-dimensional flow over horizontally homogeneous terrain. In this case an appropriate coordinate system is the rectangular Cartesian

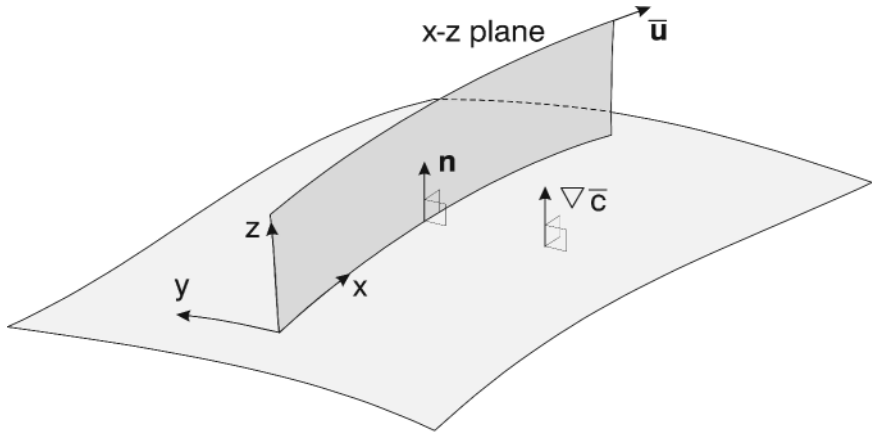

Figure 3.1. The coordinate system should be such that the local normal to the surface and the mean scalar gradient $\nabla\overline{c}$ lie in the x-z plane.

frame and with an arbitrary orientation of the axes and with velocity components u, v, w aligned with x, y, z respectively, the divergence of the mean aerodynamic flux vector becomes,

$$\nabla.\overline{\vec{u}c} = \frac{\partial\overline{uc}}{\partial x} + \frac{\partial\overline{vc}}{\partial y} + \frac{\partial\overline{wc}}{\partial z} \tag{3.2}$$

where the overbar denotes a time average.

One-dimensionality of the wind field and horizontal homogeneity of the surface scalar source impose strong symmetries on the velocity and scalar fields so that gradients of mean quantities depend only on distance from the surface. Hence, if we orient $\vec{e}_i$ so that the z axis is normal to the surface we find

$$\nabla.\overline{\vec{u}c} = 0 + 0 + \frac{\partial\overline{wc}}{\partial z} \tag{3.3}$$

In this case the divergence operator can be estimated, at least in finite difference form, from anemometers and scalar sensors on a single tower orientated along the surface-normal z axis. A more general message can be drawn from this example, however. It reminds us that the major symmetries of the wind field and the scalar source distribution determine the alignment of gradients of mean moments of the velocity and scalar fields. In fact it is the symmetry of the wind field that the natural wind system was built upon.

If we move from one-dimensional to two- and three-dimensional flows, we expect that the alignment of flow streamlines[1], which will now be space curves, and the directions in which the scalar source distribution changes most rapidly will continue to determine the strongest symmetries of the resultant mean fields and thereby the gradient of the aerodynamic flux vector. Consider for example, boundary-layer flow over gently undulating terrain with horizontal changes in scalar source strength on scales of kilometers or greater. The mean streamlines close to the surface will be approximately parallel to the ground while the gradients of mean moments of the wind and scalar fields in the surface-normal, cross-streamline direction will be much larger than streamwise gradients. Hence we can write

$$\frac{\partial \overline{wc}}{\partial z} >> \frac{\partial \overline{uc}}{\partial x}, \frac{\partial \overline{vc}}{\partial y} \tag{3.4}$$

where the x and y directions are now aligned in the streamwise direction and in the cross-stream direction parallel to the local surface, respectively. Equivalently we can say that the local normal to the surface must lie in the x-z plane (Figure 3.1). In analogy to the case of one-dimensional flows, the best approximation to the divergence that can be obtained from an alignment of anemometers along a single tower is obtained when the instruments are located in the plane spanned by the mean wind vector and the local normal to the surface.

Flows where the mean streamlines are approximately parallel to the surface and Equation 3.4 is satisfied are sometimes referred to as 'Fairly Thin Shear Layers' (FTSL) (Bradshaw, 1973). Most long-term flux study sites conform to the FTSL description, even those in complex terrain. Henceforth, we will refer to terrain where the flow satisfies FTSL criteria as 'gentle' terrain. At such locations, we can expect that measuring $\overline{wc}/\partial z$ with x tangent to the streamline and the x-z plane normal to the surface will yield the best approximation to $\nabla.\overrightarrow{uc}$ that we can obtain from instruments orientated along a single straight line. For a practical example of this see Geissbuhler et al. (2000). As the scale of variation of the mean velocity and the scalar source in the streamwise direction begins to approach that in the cross-stream direction, however,

[1]Streamlines are curves in space that are everywhere tangent to the local velocity vector. The streamlines passing through an arbitrary curve that is not itself a streamline form a stream surface. If the velocity vector $\vec{\overline{u}}$ is a time averaged quantity, then the streamlines and stream surfaces belonging to the steady vector field $\vec{\overline{u}}(\vec{x})$ are fixed in space. Solid surfaces are stream surfaces by definition, as the normal component of $\vec{\overline{u}}$ is zero at such a surface. For more complete definitions of these objects see any standard text on fluid mechanics, e. g., Batchelor (1967) and for a comment on the limitations of the concept of a stream surface see Finnigan (1990).

this approximation rapidly becomes poor. Nevertheless, at micrometeorological sites chosen to avoid the grossest inhomogeneities in topography and source distribution, the optimal coordinate system in which to write the mass balance is one whose coordinate lines are aligned as shown in Figure 3.1.

So far we have concentrated on the mass balance at a point and the *local* orientation of the coordinate lines. In practice we want to estimate the mass balance in a control volume over a representative patch of surface. To do this we need to write the mass balance in integral form, which requires us to specify the coordinate system in which we intend to represent it as this determines the geometry of the coordinate lines along which we shall integrate. In the next section we will review the properties of two candidate systems whose coordinate lines have the *local* orientation specified above.

2.2 Coordinate systems

Coordinate systems provide two essential ingredients for the mathematical description of the mass balance: they specify the magnitude and direction of a vector basis $\vec{e}_i$ in terms of which all vector and tensor quantities can be written, e. g.

$$\vec{u} = u\vec{e}_1 + v\vec{e}_2 + w\vec{e}_3 \tag{3.5}$$

u, v, w being the components of the velocity vector $\vec{u}$ in the basis $\vec{e}_i$. They also provide coordinate lines, whose intersections can be used to locate points in space and along which we integrate, e. g., we write $\vec{u}(\vec{x}) \equiv \vec{u}(x, y, z)$ meaning the value of vector $\vec{u}$ at the position labeled by distances x, y, z, respectively from the origins of the coordinate lines. The vector basis, $\vec{e}_i$ is linked to the coordinate lines. For example, $\vec{e}_1$ might be defined as the unit tangent to the x coordinate line.

Except in the simplest case of steady one-dimensional flow over a plane surface, in which case the mean streamlines are straight lines parallel to the surface, a coordinate system that has its x lines approximately parallel to and its z lines normal to the streamlines will be curvilinear. Some salient points of curvilinear coordinate systems together with some useful references are given by Finnigan (2004). In the next section we will discuss two coordinate systems in detail: rectangular Cartesian and physical streamline coordinates, which essentially bound the range of appropriate choices.

2.2.1 Rectangular Cartesian coordinates

In this familiar system the vector basis $\vec{e}_i$ is orthonormal and the coordinate lines are straight and orthogonal and everywhere parallel to $\vec{e}_i$ so that the x coordinate is parallel to $\vec{e}_1$, y is parallel to $\vec{e}_2$ and z is parallel to $\vec{e}_3$. The instantaneous mass balance equation (Equation 3.1) written in Cartesian coordinates (from now on we will drop the qualification 'rectangular') is

$$\frac{\partial c}{\partial t} + \frac{\partial uc}{\partial x} + \frac{\partial vc}{\partial y} + \frac{\partial wc}{\partial z} = S\delta(\vec{x} - \vec{x}_0) \tag{3.6}$$

and the time averaged form of this equation is

$$\overline{\frac{\partial c}{\partial t}} + \overline{u}\frac{\partial \overline{c}}{\partial x} + \overline{v}\frac{\partial \overline{c}}{\partial y} + \overline{w}\frac{\partial \overline{c}}{\partial z} + \frac{\partial \overline{u'c'}}{\partial x} + \frac{\partial \overline{v'c'}}{\partial y} + \frac{\partial \overline{w'c'}}{\partial z} = \overline{S}\delta(\vec{x} - \vec{x}_0) \tag{3.7}$$

where the overbar denotes a simple time average (Finnigan et al. 2003) and the prime denotes an instantaneous departure from the average.

An important property of rectangular Cartesian coordinates is that, once the vector basis has been defined at any point in space, its orientation and that of the coordinate lines is defined everywhere (Figure 3.2). In particular, if we determine the x, $\vec{e}_1$ direction by making it parallel to the mean velocity vector measured by a sonic anemometer on a tower and if the mean streamline at the anemometer is not parallel to the underlying surface, then the z axis cannot be normal to the surface.

2.2.2 Physical streamline coordinates

Physical streamline coordinates are defined by the flow field itself. The instantaneous flow must first be averaged in time to define a set of mean streamlines, which become the x coordinate lines. Hence a given turbulent flow field can generate different streamline coordinate frames depending upon the way the flow is averaged. Like Cartesian coordinates, streamline coordinates employ the orthonormal basis $\vec{e}_i$ but this is now orientated so that $\vec{e}_1$ is always tangent to the local streamline, $\vec{e}_2$ is aligned with the *principal normal*[2] to the streamline and $\vec{e}_3$ is aligned

[2]The principal normal to a streamline lies in the plane that is tangent to the streamline and in which the curvature of the streamline is greatest. The binormal is perpendicular to the plane spanned by the tangent and the principal normal and the three vectors, the tangent, principal normal and binormal form the orthonormal *Frenet F* . In two-dimensional flow fields the binormals and the y coordinate lines are parallel to the surface so that the z coordinate lines intersect the surface normally. Hence the physical streamline coordinates of horizontally homogeneous flow over a flat surface are just rectangular Cartesian coordinates with the z axis normal to the surface.

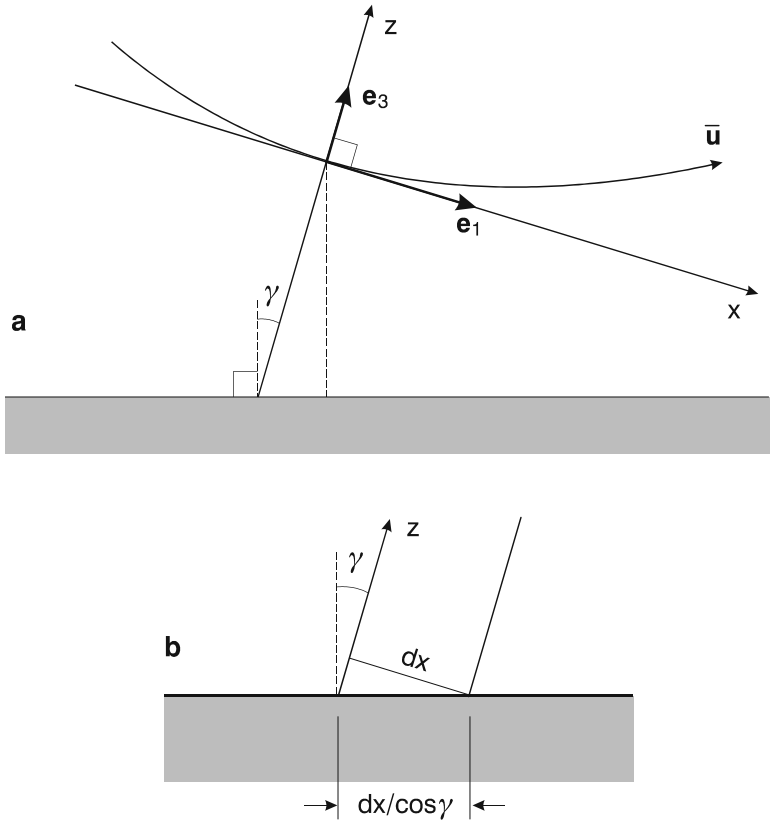

Figure 3.2. a. The orientation of a Cartesian coordinate system is determined once the base vectors are orientated at a single point, usually the anemometer position. b. If the z axis intersects the ground at an angle γ, the area of ground surface that supplies a flux of mass into the prism $\mathrm{d}x \times \mathrm{d}y \times z$ is $\mathrm{d}x \times \mathrm{d}y/\cos\gamma$.

with the binormal to the streamline (Figure 3.3). The coordinate lines x, y, z are respectively, the streamlines (x), the set of curves everywhere tangent to the binormals (y) and the set of curves everywhere parallel to the principal normals (z) (Figure 3.3). Note that in physical streamline coordinates, the y coordinate lines are associated with the $\vec{e}_3$ base vectors and the z lines with $\vec{e}_2$. This is a consequence of the micrometeorological convention where we take the positive z direction as increasing normally from the surface. Streamline coordinates are described for two-dimensional flows by Finnigan (1983) and for three-dimensional flows by Finnigan (1990) and Kaimal and Finnigan (1994). Their application to long term flux measurements is treated in much more detail in Finnigan (2004). Two-dimensional streamline coordinates have been employed

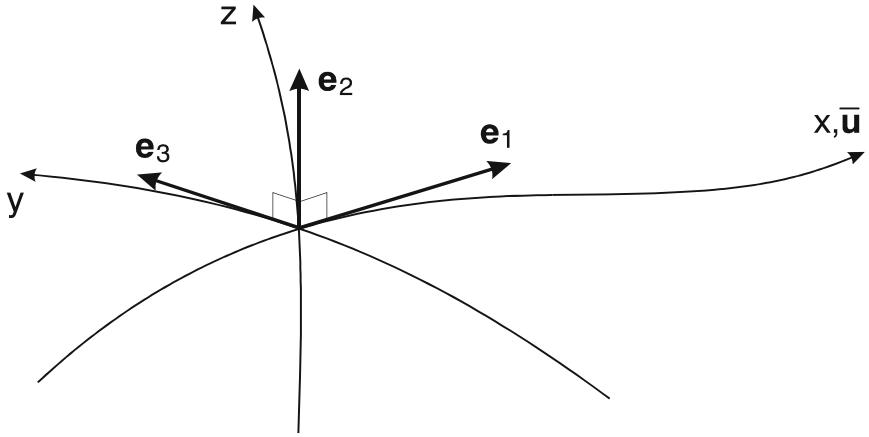

Figure 3.3. The vector basis of physical streamline coordinates is determined by the orientation of the streamline. Here $\vec{e}_1$ is the (normalized) tangent, $\vec{e}_2$ the (normalized) principal normal and $\vec{e}_3$ the (normalized) binormal to the streamline. The z coordinate lines are tangent to the field of $\vec{e}_2$ vectors and the y coordinate lines are tangent to the field of $\vec{e}_3$ vectors, while the streamlines form the x coordinates.

in analyses of complex flow fields, e. g. Finnigan and Bradley (1983), Zeman and Jensen (1984).

The time averaged mass conservation equation in three-dimensional streamline coordinates is

$$\frac{\overline{\partial c}}{\partial t} + \overline{u}\partial_x\overline{c} = -\partial_x\overline{u'c'} - \partial_y\overline{v'c'} - \partial_z\overline{w'c'} - [\frac{1}{L_a}]\overline{u'c'} + [\frac{1}{r}\frac{\partial r}{\partial y}]\overline{v'c'} - [\frac{1}{R} + \frac{1}{r}]\overline{w'c'} + S\delta(\vec{x} - \vec{x}_0) \quad (3.8)$$

where $\frac{1}{L_a} = \frac{1}{\overline{u}}\partial_x\overline{u}$, R is the local radius of curvature of the streamline and r is the local radius of curvature of the y coordinate lines. One consequence of using curvilinear systems like streamline coordinates but retaining the orthonormal vector basis $\vec{e}_i$ so variables have their familiar meaning is that the derivatives in the equations are directional rather than partial derivatives and we have written them as ∂_x, ∂_y etc. to distinguish them from partial derivatives. However, for most practical applications directional and partial derivatives are interchangeable. The main difference that needs to be kept in mind when doing mathematical manipulation of streamline coordinate equations is that derivatives along orthogonal coordinate lines do not commute so $\partial_x\partial_y\phi - \partial_y\partial_x\phi \neq 0$,

where $\phi(x, y, z)$ is an arbitrary function (Finnigan, 1990). Momentum equations and rate equations for the components of the Reynolds stresses in this coordinate frame may be found in Kaimal and Finnigan (1994).

We see in Equation 3.8 that in streamline coordinates the advection term has been simplified relative to Equation 3.7 so that only streamwise advection appears in the equation but that the flux divergence has acquired extra terms that arise because of the changing orientation of $\vec{e}_i$ in space and because the infinitesimal control volume $\mathrm{d}x\mathrm{d}y\mathrm{d}z$ changes shape as streamlines converge or diverge. On comparing the eddy flux terms in Equations 3.7 and 3.8 it is apparent that these extra terms all involve the radii of curvature of the coordinate lines.

2.2.3 Other coordinate systems

Mathematical models of flow and transport over complex terrain are often developed in various kinds of surface-following coordinate systems. See for example, Howarth (1951), Bradshaw (1973), Pielke (1984), Ferziger and Peric (1997). While these systems offer advantages for constructing models, they have significant disadvantages for interpreting tower measurements. The main ones are that the coordinate systems are generally non-orthogonal and the associated vector bases are not orthogonal unit vectors so that the dependent variables in these systems do not correspond to the physical quantities that our instruments measure. We will not discuss such systems further here. For a more detailed appreciation see Finnigan (2004).

2.3 Advantages and disadvantages of Cartesian and streamline coordinate systems

A comparison of Equations 3.7 and 3.8 shows that the mass balance expressed in streamline coordinates has a simplified advection term but a more complicated expression for the flux divergence with three extra terms to estimate. In gentle terrain it is probably easier to estimate the parameters L_a, R and r than it is to estimate the cross stream advection terms $\overline{v}\partial\overline{c}/\partial y + \overline{w}\partial\overline{c}/\partial z$ as R and r can be approximated as $R = R_0 + z$ and $r = r_0 + z$, where R_0 and r_0 are the curvatures of the surface and can be calculated from a digital elevation or contour map. In steeper topography, however, this advantage is lost and multipoint measurements are required to close the mass balance whichever coordinate frame it is written in.

Another advantage of streamline coordinates is that the vector basis $\vec{e}_i$ is everywhere aligned with the local mean wind vector $\vec{\overline{u}}$ so that a series of anemometers can be combined in the mass balance calculation

once their outputs have been rotated into the local $\vec{e}_i$ basis. In Cartesian coordinates, in contrast, once the orientation of $\vec{e}_i$ has been determined for one anemometer, it is fixed everywhere in space and the orientations of additional anemometers relative to the first must be known to use their outputs in the mass balance calculation.

To move from the time averaged mass balance at a point as expressed by Equations 3.7 and 3.8 to the integral mass balance in a control volume, we need to integrate Equations 3.7 and 3.8 over a prism whose lower face is the vegetated surface and whose aerial faces are determined by the coordinate surfaces. This raises the issue of determining these surfaces which in gentle terrain is somewhat easier in the case of streamline coordinates than in Cartesian coordinates. In steep terrain however, neither system is obviously superior to the other. A more complete treatment of the pros and cons of the two coordinate systems may be found in Finnigan (2004).

3 Coordinate Systems for Point Measurements

3.1 General considerations

This Section discusses three coordinate frames that are used most frequently for the interpretation of point eddy covariance measurements. These coordinate frames all define a local vector basis in which vector quantities such as air velocity and eddy flux are expressed. In addition, none of them uses the scalar concentration and flux fields to constrain the vector basis. This second feature is an important one because any other coordinate systems constrained in whole or in part by the scalar flux vector will give physically unrealistic results.

In Section 2, we make a distinction between the vector basis, a local property of a coordinate system, and the overall coordinate frame consisting of the vector basis and coordinate lines, a global property of the flow that is determined by the flow field in three dimensions. From an operational viewpoint, point measurements can only define the local vector basis. Even with multiple sensors, it is extremely difficult to determine coordinate lines of the global coordinate frame because the sensors can rarely be aligned relative to one another with sufficient accuracy. Furthermore, point measurements give some but not all of the terms of the surface-layer mass balance. It is therefore crucial that we work in coordinate frames that optimizes our ability to estimate surface-vegetation exchange such as NEE, using the terms we can measure. A suitable coordinate frame must also maximize information for diagnostics purposes (e. g., to answer the question of whether atmospheric conditions

are too limiting to allow a meaningful NEE estimate) and for advancing our understanding of the 3-dimensional nature of the flow.

Unfortunately, in the authors' opinion, the information produced by eddy covariance has not been fully utilized because most field studies focus too narrowly on the vertical eddy fluxes such as CO_2 flux and the streamwise momentum flux. It is known that even at ideal sites, the 30-min mean velocity vector can depart from the local terrain surface. Recovery of the mean vertical velocity may help us determine whether the observation suffers from undersampling of low frequency eddies or from the influence of mesoscale motion at scales larger than the scale of the flux footprint. It is also known that $\overline{v'w'}$, the cross-wind momentum flux, cannot be assumed to equal zero in the ocean atmospheric surface layer (Wilczak et al. 2001), at sites on rolling topography (Section 6), and at times when wind directional shear exists in the surface layer. Tanner and Thurtell (1969) pointed out that when $\overline{u'v'}$ (covariance between the streamwise and lateral velocity components) is not zero, conditions are not ideal and local divergence caused by fetch or surface inhomogeneity may be occurring. Lee (2004) discussed the mechanism of generation of the horizontal eddy flux, $\overline{u'c'}$, in the surface layer and how it can be used provide additional information on the advective influences on flux observations. These quantities are physically meaningful only if a coordinate is chosen properly.

A suitable coordinate system also provides a consistent framework for data analysis. This is especially true if one wishes to recover flux loss at low frequencies (Finnigan et al. 2003, Sakai et al. 2001, Chapter 5). In this regard, rotation at every 30 min interval, which is equivalent to high-pass filtering, produces the undesirable effect of having turbulent time series that are discontinuous. Similarly, construction of ensemble mean spectra and cospectra should be done in an appropriate coordinate frame so that the low frequency contributions to the spectra are not missed.

3.2 Instrument coordinate

This is an orthogonal coordinate frame deployed by the anemometer to express the components of the wind and the associated eddy flux vectors. In some modern designs, the transducers of the sonic anemometer are arranged non-orthogonally to minimize flow interference. Projection of the velocity vector from the non-orthogonal to the desired orthogonal frame involves straightforward geometric transformation, which is ac-

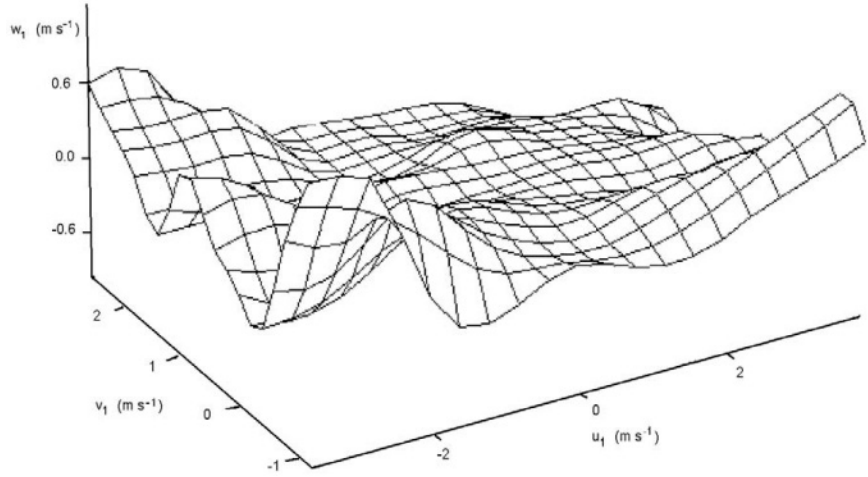

Figure 3.4. Contour plot of instrument velocity components showing the interference on air motion by the instrument tower at the Wind River site, Washington, U. S. A. (Paw U et al. 2004).

complished by firmware for the user. The geometry of the anemometer has some bearing in the way correction is made for the cross-wind effect on the sonic signal (Kaimal et al. 1990, Liu et al. 2001) and for flux loss due to pathlength averaging (Chapter 4)[3].

The base vectors of the instrument coordinate system are fixed once the position of the anemometer is known relative to some geographic reference. For example, the $\vec{e}_1$ vector may be pointing to the north, the $\vec{e}_3$ vector to the west, and the $\vec{e}_2$ vector aligned with, and in the opposite direction of, the gravitational force if the anemometer is leveled. In this sense, the instrument coordinate is an absolute one that is independent of the flow field. Micrometeorologists without exception should always archive the data of velocity statistics and flux cross products expressed in this coordinate. Although the flux cross products must undergo coordinate rotation, the velocity data themselves can be useful in many other ways. For example, the instrument velocity components can be used to determine wind direction, to infer the extent of aerodynamic interference

[3]Strictly, correction for flux loss due to pathlength averaging should be made with the velocity spectra in the non-orthogonal coordinate aligned with the separation direction of the transducers, not in any other coordinate (e. g., the natural wind system) unrelated to the geometry of the sonic anemometer design.

by the measurement platform (Figures 3.4 and 3.7), and to determine the orientation of the base vectors, in the instrument coordinate system, of the planar fit coordinate system (Appendix B).

3.3 Natural wind coordinate

Tanner and Thurtell (1969) define the natural wind coordinate system as a right-handed system in which the x-axis is parallel to the (30-min) mean flow with x increasing in the direction of the flow, the z-axis is normal to and pointed away from the underlying surface. It assumes that there is no correlation between the lateral and vertical velocities ($\overline{v'w'} = 0$). Transformation to this coordinate is accomplished by a two-step rotation procedure involving three rotation angles. For the reader's convenience, a brief account of their procedure is given in Appendix A. The complete description can be found in their original report and in McMillen (1988).

An obvious advantage of the natural wind coordinate is that by forcing the mean lateral and cross wind components to zero, it aligns the x axis to the streamline at the measurement point. In an idealized homogeneous flow, this serves the function of leveling the anemometer to the surface. It offers a consistent frame through time for periods when the anemometer position has been moved frequently.

If multiple sensors are deployed in the streamwise direction, by aligning the x axis with the local wind vector at each sensor location, measurements can be expressed in a common streamline coordinate. In Section 2, we suggest that in gentle terrain the streamline coordinate is the best frame to assess mass balance (Equation 3.8). Obviously, this is a f

Another important feature of the natural wind coordinate is that it allows online computation of the fluxes. While scalar fluxes are not particularly sensitive to tilt errors, velocity cross products in the instrument coordinate usually do not make much sense until a coordinate rotation is made. The ability to transform in real-time the velocity cross products to the streamwise momentum flux in a coordinate aligned, albeit approximately, to the surface will help the investigator detect instrument malfunction. For example, a positive covariance $\overline{u'w'}$ after rotation usually indicates problems with the sonic anemometer.

At the time of its publication, the natural wind system was intended for a surface layer in which the flow is one dimensional, and there is no wind directional shear causing cross-wind momentum flux (that is, $\overline{v'w'} = 0$). It is a suitable system for experiments conducted at ideal sites, over selected "golden days", and in homogeneous flow, fair weather

conditions. In short field campaigns at a sloped site, McMillen (1988) found that rotation to the natural wind system significantly improved his results. However, the drawbacks of the system have become apparent now that the scope of micrometeorological research has been extended considerably to include non-flat sites as well as year-round, continuous monitoring. Some of the limitations can be summarized as follows:

- *Over-rotation*: By forcing the mean vertical velocity to zero for every observational period, we run the risk of over-rotation. Section 5 gives a list of examples on when this may actually occur. Over-rotation may result in a systematic bias error in the time-integrated flux.

- *Loss of information*: Most field campaigns deploy only one eddy covariance system. The theoretical advantage of aligning the coordinate with the local wind vector is no longer compelling, since it is not possible to close the mass balance with one single sensor, and is outweighed by the disadvantage of information loss. For example, a nonzero $\overline{w}$ may exist due to thermal circulation and free convection. In rolling terrain and in direction shear (in the vertical sense) flow conditions, it is not valid to assume $\overline{v'w'} = 0$. While these quantities themselves do not permit a full mass balance closure, they offer useful information on the 3-dimensional nature of the flow influencing the measurement.

- *Degradation of data quality*: It is shown that the data quality is lower for rotation into the natural wind coordinate in comparison to the planar fit method (Chapter 9). One reason for this has to do with unrealistically large rotation angles in low wind conditions. When this occurs, the z axis is no longer in a direction along which the divergence of the eddy flux is maximized. That $\overline{v'w'} \neq$ advective flow also contributes to the problem. Finnigan (2004) points out that the third rotation angle (angle β, Appendix A) constrained by forcing $\overline{v'w'}$ to zero has a closure problem and often gives physically unrealistic results.

3.4 Planar fit coordinate

This is a right-handed orthogonal coordinate in which the z-axis is perpendicular to the mean streamline plane and the y-axis is perpendicular the plane in which the short-term (30 min) velocity vector $\vec{\overline{u}}$ and the z axis lie. The mean streamline plane is determined from an ensemble of observations made over weeks or longer. In this system the z coordinate is fixed over the chosen period, and x and y axes are variable

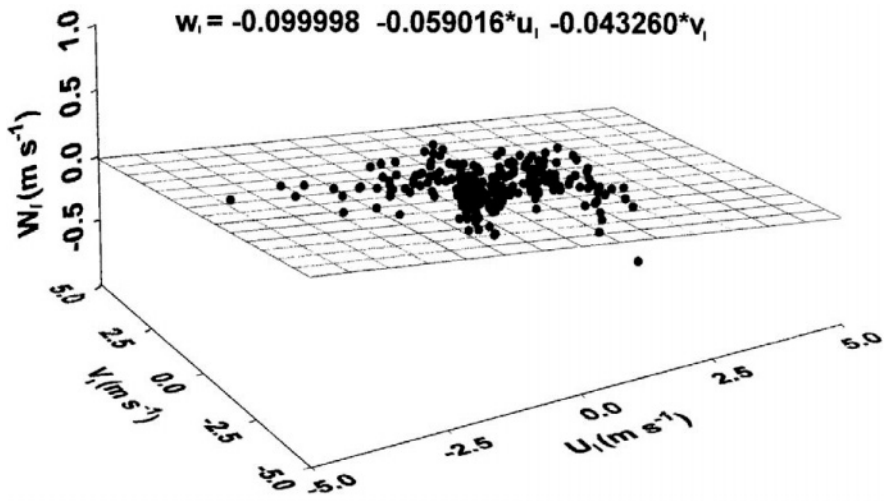

Figure 3.5. An example of planar fit regression with wind data over a maize canopy in Davis, California (Paw U et al. 2000).

with time. Strictly, the system is not a streamline coordinate because its base vectors are not aligned with the short-term mean streamline.

The steps involved in the rotation from the instrument coordinate to the planar fit coordinate are:

- Determine a period (weeks or longer) during which there was no change in the anemometer's position relative to the surface.
- Perform linear regression, $\overline{w}_1 = b_0 + b_1\overline{u}_1 + b_2\overline{v}_1$, using data from the chosen period to define a "tilted plane", or the mean streamline plane (Figure 3.5), where b_0, b_1 and b_2 are regression coefficients, and $\{\overline{u}_1, \overline{v}_1, \overline{w}_1\}$ are components of the (30-min) mean velocity in the instrument coordinate system.
- Use the regression coefficient b_1 and b_2 to determine the pitch, roll and yaw angles for rotation as in Wilczak et al. (2001) or alternatively, the base vector set that defines the three coordinate axes (Appendix B).
- Project the velocity and flux cross products into the new coordinate system.

The planar fit method overcomes some of the deficiencies of the natural wind coordinate system. The coordinate axes are not prone to

the effect of instrument offset because the offset is eliminated by the least squares procedure. The z coordinate is independent of wind direction, minimizing the problem of over-rotation in the presence of the aerodynamic shadow produced by the sensor structure (Figure 3.7). By relying on a large ensemble of observations, the coordinate frame is stable through time and the x-y plane is more or less parallel to the local surface[4]. Most importantly, with the planar fit or other similar long-term coordinates, it is possible to recover information on the 2- and 3-dimensional nature of the flow field, such as the mean vertical velocity, from observations made at a single point.

In recent years the residual mean vertical velocity in the long-term coordinate has received considerable attention. Wilczak et al. (2001) consider the residual as random noise. Lee (1998), Baldocchi et al. (2000) and Paw U et al. (2000) combine the residual with the continuity equation to estimate the contribution of vertical advection to the surface layer mass balance. Finnigan (2004) views it as being indicative of low frequency contributions to the total flux. Because it is usually small in magnitude, the mean vertical velocity is very sensitive to measurement artifacts. To recover the mean vertical velocity that is truly meteorological remains a challenging task.

Several practical considerations should be kept in mind when applying the planar fit method. Every time the sonic anemometer is moved, a new base vector set or rotation angles should be determined. The rotation method assumes that the instrument offset in the vertical velocity, if any, is constant throughout the period chosen for the coordinate determination, which is made possible by the advance in the technology of sonic anemometry. Clearly, the method should not be used in situations where the offset is not stable, or when the anemometer position has been changed too frequently. In principle, the planar fit method can be implemented in the realtime computation of fluxes providing that the base vector set has been previously determined. Finally, the influences of atmospheric stability, strong winds, and change in foliage morphology on the rotation angles remain to be investigated.

4 Flux Bias Error due to Coordinate Tilt

Let us consider once again the example of one-dimensional, non-convergent wind field and horizontal homogeneity of the surface scalar source over horizontally homogeneous terrain. According to Equations 3.1-

[4]Sites where a systematic vertical motion exists are exceptions to this. A case in point is a forest edge where the streamline is always titled at an angle from the surface (Irvine et al. 1997, Li et al. 1990).

3.3, the eddy flux $\overline{w'c'}$ is now equivalent to the true surface-air exchange. (For simplicity, we will ignore the storage correction.) Similarly, the eddy momentum flux $\overline{u'w'}$ represents the true surface shear stress. The measurement will suffer a tilt error if it is expressed in a coordinate whose vector base $\vec{e}_2$ or the z axis is tilted from the direction normal to the surface.

4.1 Momentum flux bias

The tilt error in the momentum flux has been quantified by Wilczak et al. (2001) using the mixed-layer and surface layer similarity functions. They showed that for a 1° tilt, the error is typically greater than 10% in the surface under moderately unstable conditions and can be as large as 100% under free convection conditions. The error is probably even larger in stable conditions because of poor correlation between the streamwise and vertical velocities (Kaimal and Haugen 1969). Such a bias error is highly undesirable in the context of the Monin-Obukhov similarity because friction velocity is a velocity scale and a parameter used to define the Monin-Obukhov length and the scale for the scalar concentration. This leads to the stringent requirement of an accuracy of at least 0.1° in the internal alignment and mounting of the anemometer (Kaimal and Haugen 1969).

In the context of long-term observation of surface-air exchange of energy and materials, an accurate measurement of the momentum flux will aid gap filling and data quality control. For example, friction velocity is used to screen nighttime data for well-mixed conditions (Goulden et al. 1996). If the tilt error is large, it may be difficult to establish a friction velocity threshold for CO_2 flux. Also when applying spectral corrections to the flux, one needs an accurate measurement of stability and therefore momentum flux (Chapters 4 and 5).

4.2 Scalar flux bias

To assess the scalar flux bias error, let variables with subscript 1 denote quantities in a Cartesian coordinate tilted at an angle, α, from the correct one and variables without the subscript denote quantities in the correct coordinate. Here α is positive if the instrument is tilted into the wind and negative otherwise. The vertical eddy flux in the tilted coordinate, $\overline{w_1'c'}$, can be expressed as

$$\overline{w_1'c'} = \overline{w'c'}\cos(\alpha) + \overline{u'c'}\sin(\alpha). \tag{3.9}$$

Using the following approximate relationship

$$\overline{u'c'} = a\frac{\overline{u'w'}}{\overline{w'^2}}\,\overline{w'c'} \tag{3.10}$$

to eliminate the dependence on the horizontal eddy flux, $\overline{u'c'}$ (Lee 2004), we obtain

$$\overline{w_1'c'} = \overline{w'c'}\cos(\alpha) + a\frac{\overline{u'w'}}{\overline{w'^2}}\,\overline{w'c'}\sin(\alpha). \tag{3.11}$$

Here a is an empirical constant ($a = 2.4$ and 3.3 for unstable and stable conditions, respectively). Equation 3.11 is combined with the Monin-Obukhov similarity to yield

$$\frac{\sigma_w}{u_*} = \begin{cases} 1.25(1-3z/L)^{1/3} & \text{for } z/L \le 0 \\ 1.25 & \text{for } z/L > 0 \end{cases} \tag{3.12}$$

to investigate the flux bias error (Figure 3.6), where σ_w is the vertical velocity standard deviation, u_* is friction velocity, and z/L is the Monin-Obukhov stability parameter.

Figure 3.6 shows that the scalar flux is less sensitive to sensor tilt than the momentum flux, with a tilt error usually less than 5% for small tilt angles ($\alpha < 2^\circ$). However, we should be aware of two types of systematic bias that can occur in the time integration of carbon flux. In the first, the sensor tilt angle is fixed at all times, but because the tilt error is larger in stable (nighttime) than in unstable (daytime) conditions, the overall error does not cancel out. In the second, wind direction exhibits a systematic diurnal pattern (e. g., land/sea breezes) so that the tilt angle is negative in the daytime and positive at night. This second scenario is particularly undesirable because the tilt error is of opposite sign for day versus night. If we take a typical growing season CO_2 flux of -0.5 and 0.2 $\mathrm{mg\,m^{-2}s^{-1}}$ for daytime and nighttime, respectively, and a 4% overestimation and a 5% underestimation due to a -2° and 2° tilt for daytime and nighttime, respectively (Figure 3.6), the bias in the monthly flux sum is estimated at 20 $\mathrm{g\,C\,m^{-2}}$, or on the order of 10% of the annual NEE of some temperate forests.

In this simple example of 1-dimensional flow, the global property of the coordinate system is uniquely determined by the local vector basis at the measurement location. The general conclusion is applicable in kly 2- and 3-dimensional flows. In this case, the optimal coordinate for point measurements should have its $x-z$ plane perpendicular to the local terrain surface (Figure 3.1) and the tilt error discussion should be cast in reference to this coordinate.

It should be pointed out that the above error assessment is limited to the *eddy flux* only. Errors in the overall NEE estimate caused by neglect

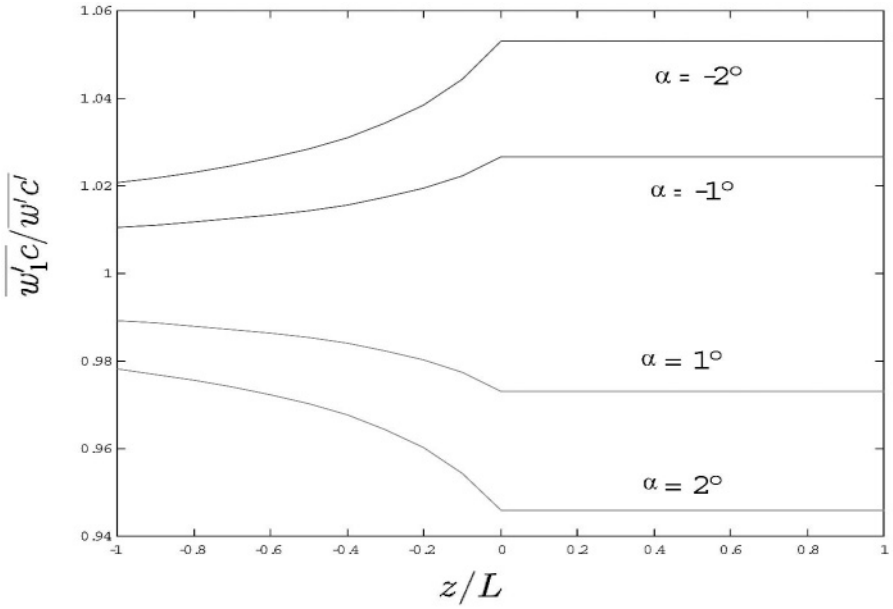

Figure 3.6. Scalar flux bias error as a function of the Monin-Obukhov stability parameter for four tilt angles.

of non-turbulent advective fluxes (e. g., $\overline{w}\,\overline{c}$) could be significantly larger in 2- and 3-dimensional flows.

5 Examples of Coordinate Tilt

Coordinate tilt can occur in several ways. The most obvious one is a physical tilt of the instrument relative to the correct coordinate frame. This can be minimized on level terrain by carefully mounting the sensor, but is unavoidable on sloped terrain because the x-y plane of an instrument leveled with respect to the geopotential is not parallel to the local terrain slope and thus is tilted from the most appropriate coordinate frame. Post-field rotation schemes attempt to remove the tilt by using wind statistics, each making a different assumption regarding the flow dynamics in the surface layer. The natural wind system assumes horizontal flow homogeneity for every observational period and thus the

velocity vector is assumed to be always parallel to the surface. A coordinate system derived from an ensemble of observations assumes that the ensemble mean velocity vector is parallel to the surface, while the velocity vector over individual observational periods can intercept the surface thus allowing non-zero mean vertical velocity.

Coordinate tilt can also occur if the instrument vertical velocity has an electronic offset. [Wilczak et al. (2001) point out that offset in the instrument horizontal velocity components is not a concern.] The instrument may be perfectly aligned with the optimal coordinate frame, but in post-field rotation, such as that of Tanner and Thurtell (1969), that forces the 30-min mean vertical velocity to zero for every observation, we end up with flux and wind statistics in an incorrect reference frame. If a typical mean velocity is 2 $\mathrm{m\,s^{-1}}$, a 5 $\mathrm{cm\,s^{-1}}$ offset in the instrument vertical velocity is equivalent to a 1.5° tilt. This "over-rotation" will introduce a bias to the integrated carbon flux especially if wind direction changes systematically from day to night. The instrument zero offset can be measured in the field by putting the anemometer in a zero wind, anechoic chamber and be removed from the signal before coordinate rotation is performed. Care should be exercised to ensure that the zero wind chamber is not subject to differential heating as to create convective motion inside. Alternatively, the offset can be removed by a least squares regression on the assumption that it remains constant over the entire experimental period (Paw U et al. 2000; Appendix B).

Another cause of coordinate tilt arises from 2- or 3-dimensional air motion. If there is horizontal flow convergence/divergence, the (30-min) mean velocity vector will no longer parallel to the terrain surface. Once again, a tilt error will result from the mean vertical velocity being forced to zero by post-field rotation. In this regard, a coordinate system based on velocity data obtained over long periods is more robust, particularly at times of low wind speed when the natural wind system often gives unrealistically large rotation angles.

The anemometer supporting frame and the instrument tower can deflect the flow to the extent that can lead to a tilted coordinate in post-field data analysis. Figure 3.7 shows an example of this problem. The tilt factor b was determined by linear regression of the instrument mean vertical velocity, $\overline{w}_1$, against the instrument horizontal velocity, $\overline{u}_1$ in

$$\overline{w}_1 = a + b\overline{u}_1, \tag{3.13}$$

over successive 15° wind direction bins (Lee 1998). The sinusoidal behavior of b as a function of wind direction, expected for the ideal case of flow free of aerodynamic interference, was not observed, suggesting the aerodynamic shadow effect on the measurement. In fact, the 120°

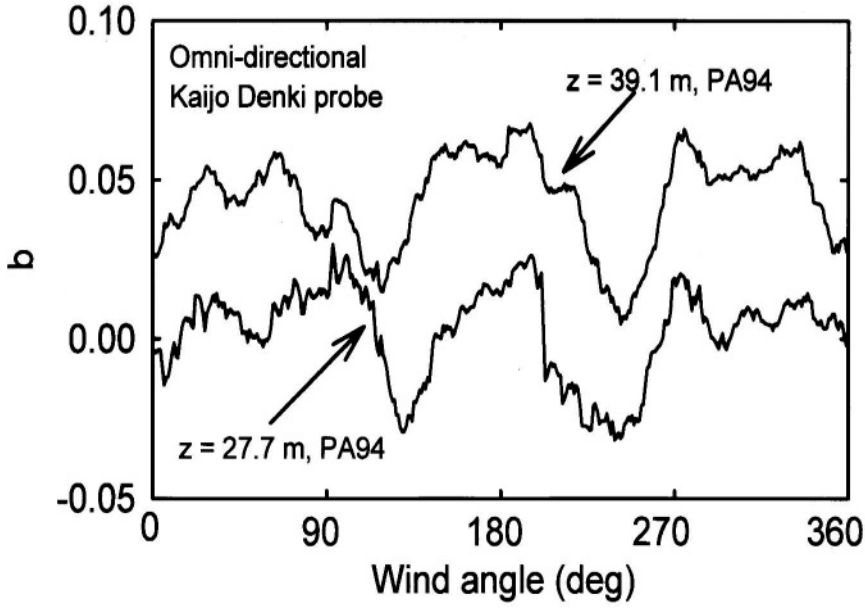

Figure 3.7. Vertical tilt factor as a function of wind direction for omnidirectional Kaijo Denki sonic anemometers at two measurements heights in a boreal aspen forest in Prince Albert, Saskatchewan, Canada.

repetitive pattern shown in Fig 3.7 corresponds to the three vertical supporting frames of the anemometer arranged 120° apart. According to Figure 3.7, by forcing the mean velocity to zero, the natural wind system can tilt the coordinate by as much as 3°. A reasonable solution to this problem is the planar fit method discussed above, which uses the data from all wind directions to determine a more stable reference frame independent of wind direction.

Finally, forcing the cross-wind momentum flux $\overline{v'w'}$ to zero may result unrealistically large rotation angles (Section 6). The tilt error in this case arises from contamination of the vertical flux $\overline{w'c'}$ by the cross-wind flux $\overline{v'c'}$ (Equation 3.17), and is usually much smaller than that arising from contamination by the streamwise flux $\overline{u'c'}$ (Equation 3.9).

6 Analysis of a Sample Dataset

6.1 Dataset

In this Section, we use a dataset obtained over the Great Mountain Forest in rolling terrain to investigate the effect of coordinate rotation

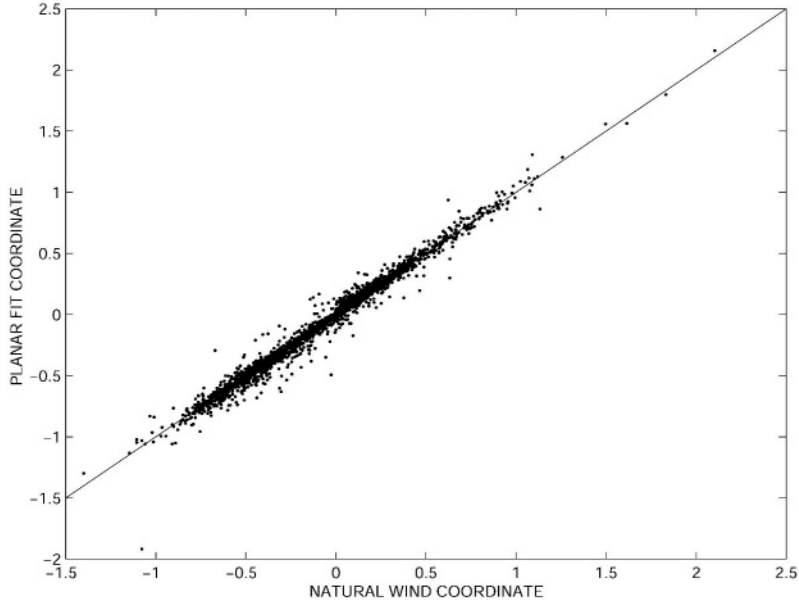

Figure 3.8. Comparison of CO_2 flux ($\mathrm{mg\,m^{-2}\,s^{-1}}$) in the natural wind and planar fit coordinates. Solid line represents 1:1.

on the flux measurement. A detailed description of the site and measurement system is given by Lee and Hu (2002). Briefly, the eddy covariance system was mounted at a height of 30.4 m, roughly 10 m above the treetops. The data obtained over June to July, 1999 was used in this analysis. The 30-min velocity and flux cross product matrix was first computed in the instrument coordinate and then transformed to the natural wind coordinate system. Rotation into the planar fit coordinate was carried out in the post field analysis. Over this period, the unit vector in the direction of the z axis of the planar fit coordinate was $\{0.060, -0.078, 0.990\}$ (Appendix B). Density corrections were applied to carbon and water vapor fluxes in all three coordinate systems.

6.2 Results

Figures 3.8 and 3.9 compare the CO_2 flux and the streamwise momentum flux in the natural wind and planar fit coordinate systems. Although statistically the slope of the regression is not different from the 1:1 line, some scatter is evident. The time integrated C flux over the two month period was -84.4, -84.8 and -88.1 $\mathrm{g\,C\,m^{-2}}$ in the instrument, natural

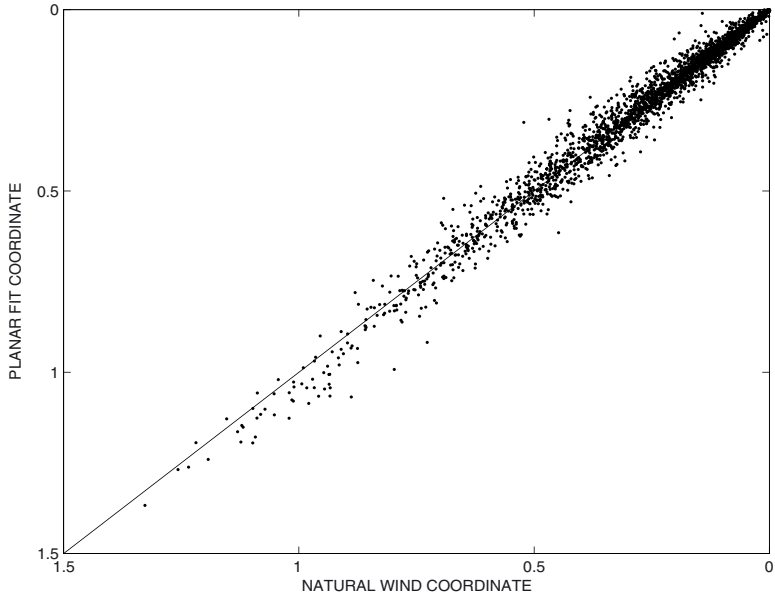

Figure 3.9. Comparison of the streamwise momentum flux ($\overline{u'w'}$, $\mathrm{m^2\,s^{-2}}$) in the natural wind and planar fit coordinates. Solid line represents 1:1.

wind, and planar fit coordinate, respectively, with a relative difference of 4%.

Figure 3.10 shows that the cross-wind momentum flux $\overline{v'w'}$ in the planar fit coordinate is usually not negligible. This is not a surprise for a surface layer over rolling topography. That $\overline{v'w'}$ is dependent upon wind direction also suggests some tower interference with the measurement. Forcing $\overline{v'w'}$ to zero would require an additional rotation of the $z-y$ plane around the x axis by as much as 20°.

To simulate the natural wind rotation scheme, we perform one additional rotation of the velocity and flux cross products in the planar fit coordinate by forcing the cross-wind momentum flux to zero. The results are given in Figures 3.11 and 3.12. Much of the scatter in Figures 3.8 and 3.9 is eliminated by the additional rotation. The R^2 value is improved from 0.983 to 0.997 for CO_2 flux and from 0.979 to 0.991 for momentum flux. Thus the primary difference between the two coordinates is the third rotation of the natural wind system that forces $\overline{v'w'}$ to zero. A rotation angle as large as 20° is clearly not physical. Fortunately, the error caused by this rotation (rotation of the $z-y$ plane around the x axis) is much smaller than the error caused by sensor tilt

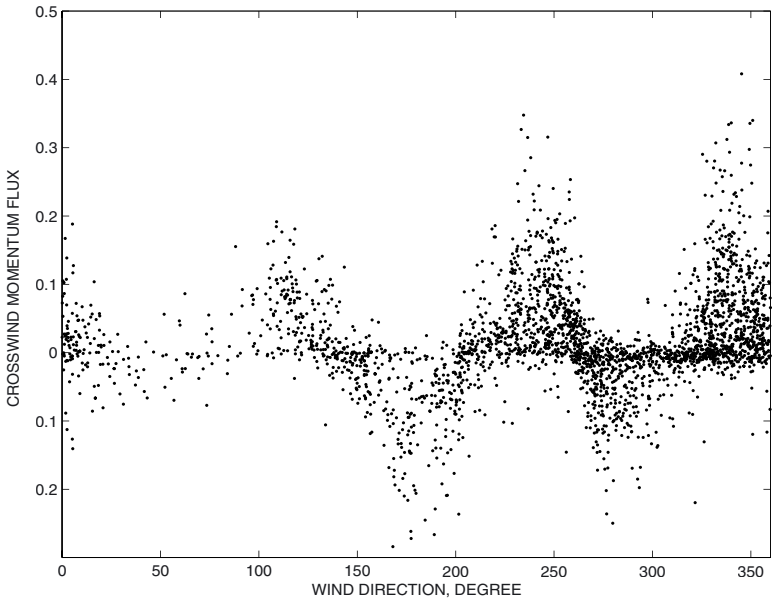

Figure 3.10. Cross-wind momentum flux ($\overline{v'w'}$, $\mathrm{m^2\,s^{-2}}$) in the planar fit coordinate as a function of wind direction.

in the streamwise direction discussed in Section 4. This is because the cross-wind scalar flux, $\overline{v'c'}$, and momentum flux, $\overline{v'w'}$, are much smaller than their streamwise counterparts, $\overline{u'c'}$ and $\overline{u'w'}$.

7 Conclusions

To convert measurement of wind speed, eddy flux and scalar concentration into estimates of the true surface-air exchange, we implicitly or explicitly assimilate the measurement into mathematical statements of the mass balance over a representative patch of the surface. The form of these statements depends on the coordinate system in which it is written and the coordinate system should be chosen so that the measurements can be used optimally. A comparative analysis of some candidate coordinate systems is performed, with a particular emphasis on the Cartesian and physical streamline systems.

In our theoretical analysis, we make a distinction between the vector basis, a local property of a coordinate system, and the overall coordinate frame consisting of the vector basis and coordinate lines, a global property of the flow that is determined by the flow field in three dimensions. Usually only a single tower is available as measurement platform. Such

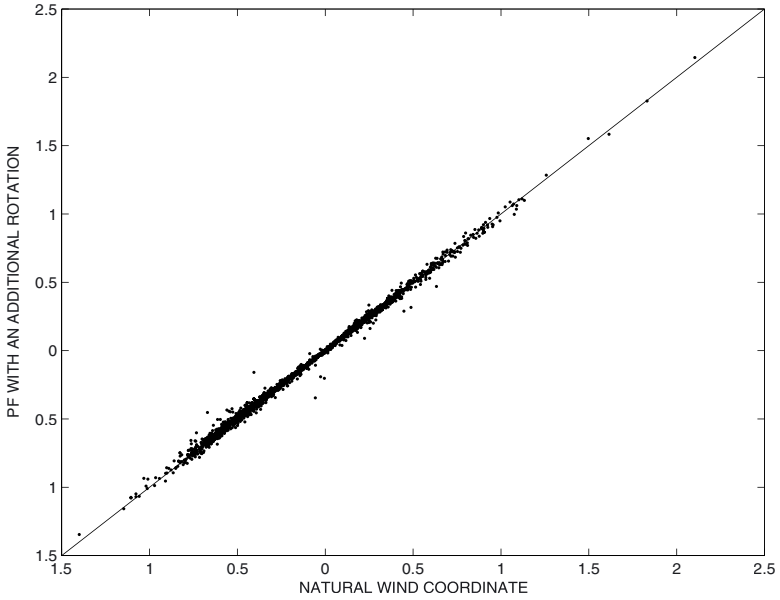

Figure 3.11. Comparison of CO_2 flux ($\mathrm{mg\,m^{-2}\,s^{-1}}$) in the natural wind coordinate and the planar fit (PF) coordinate with one additional rotation that forces $\overline{v'w'}$ to zero. Solid line represents 1:1.

point measurements can only define the vector basis, and many components that enter into the mass balance in complex flows are severely under-sampled. A suitable coordinate frame for point measurements must optimize our estimates of the surface-air exchange using the terms we can measure, and maximize information for diagnostics purposes.

We analyze the strengths and weaknesses of three operational coordinate systems for point measurements (instrument, natural wind, and planar fit). Results of the analysis of a sample dataset shows that the cumulative C flux is 4% higher in magnitude in the planar fit coordinate than in the natural wind coordinate. The difference in the eddy fluxes in the two coordinates results primarily from the third rotation performed by the natural wind system that forces $\overline{v'w'}$ to zero.

Coordinate tilt can occur in a number of ways. Besides the obvious physical tilt of the anemometer relative to the local terrain surface, coordinate tilt can easily result from post-field data analysis. Tilt error in the eddy scalar flux $\overline{w'c'}$ arises from contamination by the streamwise flux $\overline{u'c'}$ and the cross-wind flux $\overline{v'c'}$, the former of which is much larger in magnitude. That the scalar flux tilt error is usually small for small tilt

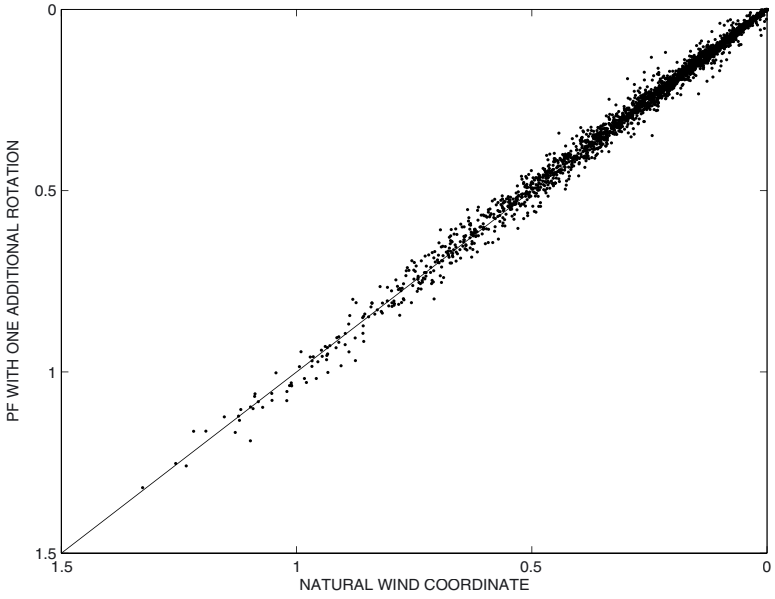

Figure 3.12. As in Figure 3.11 but for the streamwise momentum flux ($\overline{u'w'}$, $\mathrm{m^2\,s^{-2}}$).

angles does not negate the need for coordinate rotation. At sites where wind direction exhibits a systematic diurnal pattern, the time integrated C flux can suffer a systematic bias error on the order of 20 $\mathrm{g\,C\,m^{-2}}$ per month for a 2° tilt in the streamwise direction.

8 Appendix A: The Natural Wind Coordinate System

Let subscript 1 the denote velocity components and coordinate axes in the instrument coordinate. To force the mean lateral and vertical velocities to zero, we rotate through an angle η around the z_1-axis and an angle θ around the y_1-axis. The instant velocity components after the rotation, denoted with subscript 2, are

$$\begin{aligned} u_2 &= u_1(\mathrm{CT})(\mathrm{CE}) + v_1(\mathrm{CT})(\mathrm{SE}) + w_1(\mathrm{ST}) \\ v_2 &= v_1(\mathrm{CE}) - u_1(\mathrm{SE}) \\ w_2 &= w_1(\mathrm{CT}) - u_1(\mathrm{ST})(\mathrm{CE}) - v_1(\mathrm{ST})(\mathrm{SE}) \end{aligned} \tag{3.14}$$

where

$$(\mathrm{CE}) = \cos\eta \equiv \overline{u}_1/(\overline{u}_1^2 + \overline{v}_1^2)^{1/2}$$

$$\begin{aligned}(\mathrm{SE}) = \sin\eta &\equiv \overline{v}_1/(\overline{u}_1^2 + \overline{v}_1^2)^{1/2} \\ (\mathrm{CT}) = \cos\theta &\equiv (\overline{u}_1^2 + \overline{v}_1^2)^{1/2}/(\overline{u}_1^2 + \overline{v}_1^2 + \overline{w}_1^2)^{1/2} \\ (\mathrm{ST}) = \sin\theta &\equiv \overline{w}_1/(\overline{u}_1^2 + \overline{v}_1^2 + \overline{w}_1^2)^{1/2}\end{aligned} \tag{3.15}$$

To force $\overline{w'v'}$ to zero, we must rotate the intermediate z_2-y_2 plane through an angle β. After this third rotation, we obtain

$$\begin{aligned}u &= u_2 \\ v &= v_2(\mathrm{CB}) + w_2(\mathrm{SB}) \\ w &= w_2(\mathrm{CB}) - v_2(\mathrm{SB})\end{aligned} \tag{3.16}$$

where

$$\begin{aligned}\mathrm{CB} &= \cos\beta \\ \mathrm{SB} &= \sin\beta\end{aligned}$$

and

$$\beta = \frac{1}{2}\tan^{-1}\left[\frac{2\overline{v_2'w_2'}}{(\overline{v_2'^2} - \overline{w_2'^2})}\right]$$

By performing Reynolds decomposition and averaging, we can determine the velocity cross products and the flux vector in the natural coordinate from those reported in the instrument coordinate. For example, the vertical flux of scalar c is

$$\overline{w'c'} = \overline{w_2'c'}(\mathrm{CB}) - \overline{v_2'c'}(\mathrm{SB}) \tag{3.17}$$

where

$$\begin{aligned}\overline{w_2'c'} &= \overline{w_1'c'}(\mathrm{CT}) - \overline{u_1'c'}(\mathrm{ST})(\mathrm{CE}) - \overline{v_1'c'}(\mathrm{ST})(\mathrm{SE}) \\ \overline{v_2'c'} &= \overline{v_1'c'}(\mathrm{CE}) - \overline{u_1'c'}(\mathrm{SE})\end{aligned}$$

9 Appendix B: An Alternative Method for Rotation into the Planar Fit Coordinate

In Wilczak et al. (2001), rotation into the planar fit coordinate is accomplished by three successive steps according to pitch, roll and yaw angles. The sequence of rotation cannot be mixed. Here in the spirit of the base vector operation (Section 2), we outline an alternative approach, related to Paw U et al.'s (2000) 2-D planar fit regression. Our approach first determines the base vectors for the planar fit coordinate and then projects the measured vector quantities (velocity, flux) to each of the

base vectors. This scheme relies on the straightforward vector operation and avoids the need for rotation angles and thus rotation sequence is irrelevant.

Let the unit vector set $\{\vec{i}, \vec{j}, \vec{k}\}$ define the desired right-handed orthogonal coordinate such that $\vec{i}$, $\vec{j}$ and $\vec{k}$ are parallel to its x, y and z axes, respectively[5]. Thus, the mean vertical velocity in this coordinate is the inner product of $\vec{k}$ and the mean velocity vector $\vec{\overline{u}}$

$$\overline{w} = \vec{k} \cdot \vec{\overline{u}}. \tag{3.18}$$

Substituting the component forms of the two vectors in the *instrument* coordinate

$$\vec{k} = \{k_1, k_2, k_3\},\ \vec{\overline{u}} = \{\overline{u}_1, \overline{v}_1, \overline{w}_1 - b_0\},$$

into Equation 3.18 and solving for $\overline{w}_1$, we obtain

$$\overline{w}_1 = b_0 + b_1\overline{u}_1 + b_2\overline{v}_2 + \overline{w}/k_3. \tag{3.19}$$

The coefficients in Equation 3.19, b_0 (instrument offset in the vertical velocity), $b_1(= -k_1/k_3)$ and $b_2(= -k_2/k_3)$ are determined using a least squares regression procedure on the assumption that the last term represents "random noise". The components of $\vec{k}$ can be determined once b_1 and b_2 are known (see Matlab function unit_vector_k below).

Next we know that the y axis is perpendicular to $\vec{k}$ by definition of an orthogonal coordinate, and to $\vec{\overline{u}}$ so that after rotation the mean lateral velocity vanishes. Thus

$$\vec{j} = \vec{k} \times \vec{\overline{u}}/|\vec{k} \times \vec{\overline{u}}|. \tag{3.20}$$

Also by definition of a right-handed orthogonal coordinate, we have

$$\vec{i} = \vec{j} \times \vec{k}.$$

(Matlab function unit_vector_ij).

After all the three unit base vectors are known, the fluxes and velocity statistics can be projected easily onto the appropriate axes (Matlab functions scalar_ flux and velocity_stat). For example, the vertical scalar flux is the inner product of the flux vector and vector $\vec{k}$

$$\overline{w'c'} = \{\overline{u'_1c'}, \overline{v'_1c'}, \overline{w'_1c'}\} \cdot \vec{k}$$

[5]The vector set $\{\vec{i}, \vec{j}, \vec{k}\}$ is the same as $\{\vec{e}_1, \vec{e}_3, \vec{e}_2\}$ in the main text. We change the notation here for convenience of coding the routine.

```
% determines unit vector k (parallel to new z-axis)
% input
%    U1(:,1):  mean u1 in instrument coordinate
%      (:,2):  mean v1 in instrument coordinate
%      (:,3):  mean w1 in instrument coordinate
% output
%    k:  unit vector parallel to new coordinate z axis
%    b0:  instrument offset in w1
%
function [k,b0]=unit_vector_k(U1)
% wilczak's routine
u=(U1(:,1))'; v=(U1(:,2))'; w=(U1(:,3))';
flen=length(u);
su=sum(u); sv=sum(v); sw=sum(w); suv=sum(u*v'); suw=sum(u*w');
svw=sum(v*w'); su2=sum(u*u'); sv2=sum(v*v');
H=[flen su sv; su su2 suv; sv suv sv2]; g=[sw suw svw]';
x=H\g; b0=x(1); b1=x(2); b2=x(3);
%
% determine unit vector k
k(3)=1/(1+b1^2+b2^2)^0.5;
k(1)=-b1*k(3);
k(2)=-b2*k(3);
return;

% determines unit vectors i, j (parallel to new coordinate x and y axes)
%
% input
%    U1(1):  (30-min) mean u1 in instrument coordinate
%      (2):  v1 in instrument coordinate
%      (3):  w1 in instrument coordinate
%    k:  unit vector parallel to the new coordinate z-axis
% output
%    i, j:  unit vector parallel to new coordinate x and y axes
%
function [i,j]=unit_vector_ij(U1,k)
j=cross(k,U1); j=j/(sum(j.*j))^0.5; i=cross(j,k);
return;

% determines scalar flux in new coordinate
%
% input
%    u1c,v1c,w1c:  scalar flux in instrument coordinate
%    i, j, k:  unit vectors parallel to the new coordinate x, y and
% z-axes output
%    uc,vc,wc:  scalar flux in new coordinate
%
function [uc,vc,wc]=scalar_flux(u1c,v1c,w1c,i,j,k)
H=[u1c v1c w1c]; uc=sum(i.*H); vc=sum(j.*H); wc=sum(k.*H);
```

```
return;


% determines velocity statistics in new coordinate
%input
%    u:  3 by 3 matrix of cross product of the three velocity components
%      (u(1,1) = u1^u1, u(1,2)=u1^v1, etc.)  in instrument coordinate
%      i, j, k:  unit vectors parallel to the new coordinate x, y and
% z-axes output
%    uu, vv, ww, uw, vw:  statistics in new coordinate
%
function [uu,vv,ww,uw,vw]=velocity_stat(u,i,j,k)
uu=i(1)^2*u(1,1)+i(2)^2*u(2,2)+i(3)^2*u(3,3)+...
2*(i(1)*i(2)*u(1,2)+i(1)*i(3)*u(1,3)+i(2)*i(3)*u(2,3));
vv=j(1)^2*u(1,1)+j(2)^2*u(2,2)+j(3)^2*u(3,3)+...
2*(j(1)*j(2)*u(1,2)+j(1)*j(3)*u(1,3)+j(2)*j(3)*u(2,3));
ww=k(1)^2*u(1,1)+k(2)^2*u(2,2)+k(3)^2*u(3,3)+...
2*(k(1)*k(2)*u(1,2)+k(1)*k(3)*u(1,3)+k(2)*k(3)*u(2,3));
uw=i(1)*k(1)*u(1,1)+i(2)*k(2)*u(2,2)+i(3)*k(3)*u(3,3)+...
(i(1)*k(2)+i(2)*k(1))*u(1,2)+(i(1)*k(3)+i(3)*k(1))*u(1,3)+...
(i(2)*k(3)+i(3)*k(2))*u(2,3);
vw=j(1)*k(1)*u(1,1)+j(2)*k(2)*u(2,2)+j(3)*k(3)*u(3,3)+...
(j(1)*k(2)+j(2)*k(1))*u(1,2)+(j(1)*k(3)+j(3)*k(1))*u(1,3)+...
(j(2)*k(3)+j(3)*k(2))*u(2,3);
return;
```

10 Acknowledgment

The first and third authors acknowledge support by the Biological and Environmental Research Program (BER), U. S. Department of Energy, through the National Institute for Global Environmental Change (NIGEC) under Cooperative Agreement No. DE-FC03-90ER61010. Additional support was provided by the U. S. National Science Foundation through grant ATM-0072864 (to the first author).

11 References

Batchelor, G. K.: 1967, *An Introduction to Fluid Mechanics*, Cambridge University Press, New York.

Baldocchi, D., Finnigan, J., Wilson, K., Paw U, K. T.: 2000, 'On measuring net ecosystem carbon exchange over tall vegetation in complex terrain', *Bound.-Layer Meteorol.* **96**, 257-291.

Bradshaw, P.: 1973, 'Effects of streamline curvature on turbulent flow', *AGARDograph No. 169*, National Technical Information Service, US Dept. of Commerce, pp. 125.

Ferziger, J. H., Peric, M.: 1997, *Computational Methods for Fluid Dynamics*, Springer-Verlag, Berlin.

Finnigan, J. J.: 2004, 'A re-evaluation of long-term flux measurement techniques. Part II: coordinate systems', *Bound.-Layer Meteorol.* in review.

Finnigan, J. J., Clements, R., Malhi, Y., Leuning, R., Cleugh, H.: 2003, 'A re-evaluation of long-term flux measurement techniques. Part I: averaging and coordinate rotation', *Bound.-Layer Meteorol.* **107**, 1-48.

Finnigan, J. J.: 1990, 'Streamline coordinates, moving frames, chaos and integrability in fluid flow', *Topological Fluid Mechanics, Proc. IUTAM Symp. Topological Fluid Mechanics*, Eds Moffat, H. K., Tsinober A., Cambridge University Press, Cambridge, 64-74.

Finnigan, J. J.: 1983, 'A streamline coordinate system for distorted two-dimensional shear flows', *J. Fluid Mech.* **130**, 241-258.

Finnigan, J. J., Bradley, E. F.: 1983, 'The turbulent kinetic energy budget behind a porous barrier: an analysis in streamline coordinates', *J. Wind Eng. Ind. Aerodyn.* **15**, 157-168.

Geissbuhler, P., Siegwolf, R., Eugster, W.: 2000, 'Eddy covariance measurements on mountain slopes: the advantage of surface-normal sensor orientation over a vertical set-up', *Bound.-Layer Meteorol.* **96**, 371-392.

Goulden, M. L., Munger, J. W., Fan, S.-M., Daube, B. C., Wofsy, S. C.: 1996, 'Measurements of carbon sequestration by long-term eddy covariance methods and a critical evaluation of accuracy', *Global Change Biology* **2**, 169-183.

Howarth, L.: 1951, 'The boundary-layer in three dimensional flow. Part I: derivation of the equations for flow along a general curved surface', *Phil. Mag.* **42**, 239-243.

Irvine, M. R., Gardiner, B. A., Hill, M. K.: 1997, 'The evolution of turbulence across a forest edge', *Bound.-Layer Meteorol.* **94**, 467-497.

Kaimal, J. C., Finnigan, J. J.: 1994, *Atmospheric Boundary Layer Flows: Their Structure and Measurement*, Oxford University Press, New York.

Kaimal, J. C., Gaynor, J. E., Zimmerman, H. A., Zimmerman, G. A.: 1990, 'Minimizing flow distortion errors in a sonic anemometer', *Bound.-Layer Meteorol.* **53**, 103-115.

Kaimal, J. C., Haugen, D. A.: 1969, 'Some errors in the measurement of Reynolds stress', *J. Appl. Meteorol.* **8**, 460-462.

Lee, X.: 2004, 'Forest-atmosphere exchanges in non-ideal conditions: the role of horizontal eddy flux and its divergence' *Forest at the Land-Atmosphere Interface* (Mencuccini, M. et al. Eds), CAB International, pp145-157.

Lee, X., Hu, X.: 2002, 'Forest-air fluxes of carbon and energy over non-flat terrain', *Bound.-Layer Meteorol.* **103**, 277-301.

Lee, X.: 1998, 'On micrometeorological observations of surface-air exchange over tall vegetation', *Agric. Forest Meteorol.* **91**, 39-49.

Li, Z., Lin, J. D., Miller, D. R.: 1990, 'Air flow over and through a forest edge: a steady state numerical simulation', *Bound.-Layer Meteorol.* **51**, 179-197.

Liu, H. P, Peters, G., Foken, T.: 2001, 'New equations for sonic temperature variance and buoyancy heat flux with an omnidirectional sonic anemometer', *Bound.-Layer Meteorol.* **100**, 459-468.

Massman, W. J., Lee, X.: 2002, 'Eddy covariance flux corrections and uncertainties in long-term studies of carbon and energy exchanges', *Agric. Forest Meteorol.* **113**, 121-144.

McMillen, R. T.: 1988, 'An eddy correlation technique with extended applicability to non-simple terrain', *Bound.-Layer Meteorol.* **43**, 231-245.

Paw U, K. T., Baldocchi, D., Meyers, T. P., Wilson, K. B.: 2000, 'Correction of eddy-covariance measurements incorporating both advective effects and density fluxes', *Bound.-Layer Meteorol.* **97**, 487-511.

Paw U, K. T., Falk, M., Suchanic, T. H., Ustin, S. L., Chen, J., Park, Y.-S., Winner, W. E., Thomas, S. C., Hsiao, T. C., Shaw, R. H., King, T. S., Pyles, R. D., Schroeder, M., Matista, A. A.: 2004, 'Carbon dioxide exchange between an old growth forest and the atmosphere', *Ecosystems*, in press.

Pielke, R. A.: 1984, *Mesoscale Meteorological Modeling*, Academic Press, New York.

Raupach, M. R.: 2001 'Inferring Biogeochemical sources and sinks from atmospheric concentrations: general considerations and applications in vegetation canopies', In Shulze, E-D., Heimann, M., Harrison, S., Holland, E., Lloyd, J., Prentice, I. C., Schimel, D. (Eds) *Global Biogeochemical Cycles in the Climate System* , Academic Press, 41-59.

Sakai, R. K., Fitzjarrald, D. R., Moore, K. E.: 2001, 'Importance of low-frequency contributions to eddy fluxes observed over rough surfaces', *J. Appl. Meteorol.* **40**, 2178-2192.

Tanner, C. B., Thurtell, G. W.: 1969, 'Anemoclinometer measurements of Reynolds stress and heat transport in the atmospheric surface layer', *Research and Development Tech. Report ECOM 66-G22-F to the US Army Electronics Command*, Dept. Soil Science, Univ. of Wisconsin, Madison, WI.

Wilczak, J. M., Oncley , S. P., Sage, S. A.: 2001, 'Sonic anemometer tilt correction algorithms', *Bound.-Layer Meteorol.* **99**, 127-150.

Zeman, O., Jensen, N. O.: 1987, 'Modification of turbulence characteristics in flow over hills", *Quart. J. Roy Meteorol. Soc.* **113**, 55-80.